Electrokinetic Migration of Nitrate Through Heterogeneous Granular Porous Media

by Richard T. Gill, Steven F. Thornton, Michael J. Harbottle, and Jonathan W.N. Smith

Abstract

This study investigates and quantifies the influence of physical heterogeneity in granular porous media, represented by materials with different hydraulic conductivity, on the migration of nitrate, used as an amendment to enhance bioremediation, under an electric field. Laboratory experiments were conducted in a bench-scale test cell under a low applied direct current using glass bead and clay mixes and synthetic groundwater to represent ideal conditions. The experiments included bromide tracer tests in homogeneous settings to deduce controls on electrokinetic transport of inorganic solutes in the different materials, and comparison of nitrate migration under homogeneous and heterogeneous scenarios. The results indicate that physical heterogeneity of subsurface materials, represented by a contrast between a higher-hydraulic conductivity and lower-hydraulic conductivity material normal to the direction of the applied electric field exerts the following controls on nitrate migration: (1) a spatial change in nitrate migration rate due to changes in effective ionic mobility and subsequent accumulation of nitrate at the interface between these materials; and (2) a spatial change in the voltage gradient distribution across the hydraulic conductivity contrast, due to the inverse relationship with effective ionic mobility. These factors will contribute to higher mass transport of nitrate through low hydraulic conductivity zones in heterogeneous porous media, relative to homogeneous host materials. Overall electrokinetic migration of amendments such as nitrate can be increased in heterogeneous granular porous media to enhance the in situ bioremediation of organic contaminants present in low hydraulic conductivity zones.

Introduction

The effectiveness of groundwater remediation using hydraulic-based techniques is limited in aquifers and sediments with a hydraulic conductivity (K) less than about 10^{-7} m/s (Saichek and Reddy 2005a). In low K porous media solute transport may be influenced more by diffusion than advection. This can result in the sequestration of contaminants within low K zones (e.g., clays and silts) in settings characterised by physical heterogeneity (e.g., K contrasts), making them inaccessible to treatments delivered by hydraulic methods, such as amendment injection (Li et al. 2010), or those involving fluid extraction, such as pump and treatment (Lee et al. 2000). The low K zones then function as secondary sources of contaminants, which diffuse back into more permeable zones, prolonging remediation measures (Reynolds and Kueper 2002). Electrokinetics (EK) can initiate different transport phenomena (electroosmosis, electromigration, and electrophoresis) in porous media with hydraulic conductivities as low as 10^{-10} m/s (Acar and

Alshawabkeh 1993; Reddy and Saichek 2003). Coupling these processes to the delivery of suitable amendments may therefore enhance the treatment of contaminants within low K strata, using techniques such as bioremediation. This can be achieved by overcoming technical barriers for bioremediation (Gill et al. 2014), for example: (1) electromigration or electroosmotic delivery of electron acceptors and nutrients to the contaminant and/or microorganisms to overcome mass transfer limitations (Lohner et al. 2008); (2) increasing the bioaccessible contaminant fraction by enhancing desorption by electroosmotic pore fluid flux (Niqui-Arroyo et al. 2006); and (3) augmenting the indigenous microbial community to enhance species diversity and increase the biodegradation capacity (Mao et al. 2012).

Most studies of EK applications have been conducted in homogeneous rather than heterogeneous materials, although the latter more appropriately represent the subsurface environment. In many cases physical heterogeneity, represented by spatial variability in the distribution and form of materials with different K, exerts a significant control on solute transport (Song et al. 2014), contaminant distribution (Rahman et al. 2005) and options for remediation strategies in soils and aquifers (McCray et al. 2011). EK-moderated transport of substances into, and out of, low K zones in a heterogeneous setting can be significantly more effective than advection (Saichek and Reddy 2005b; Reynolds et al. 2008). However, to date there are no empirical studies of the influence of physical heterogeneity on EK transport. Nitrate is often used as an amendment to support the in

situ bioremediation of organic chemicals in contaminated aquifers, because it is less affected by solubility limitations (unlike oxygen) and can support the anaerobic biodegradation of a wide range of organic compounds (Spence et al. 2001; Bauer et al. 2008; Xu et al. 2010). However, the performance of bioremediation can be significantly limited due to the effect that physical heterogeneity exerts on the distribution and mixing of microbes and solutes in the subsurface (Song and Seagren 2008). Therefore, if the migration and bioavailability of an amendment across a K boundary where advection is significantly reduced can be increased using EK transport processes, biodegradation rates for bioremediation may be enhanced in these scenarios.

The aim of this study was to investigate the influence of K contrasts, as a form of physical heterogeneity in granular porous media, on the electromigration of an inorganic chemical which may be used as an amendment to enhance bioremediation in situ. The objectives were to:

1. Compare the migration of the amendment under homogeneous and heterogeneous conditions represented by a K contrast normal to the direction of the electric field, using nitrate as a model inorganic compound;
2. Determine the effect of physical heterogeneity described in (1) on an amendment applied at different concentrations, and;
3. Determine the effect of varying the K contrast described in (1) on the amendment mass flux and distribution of the voltage gradient.

Currently no studies have quantified the effect of K contrasts on amendment mass flux or voltage gradient distribution for EK applications. This is an important knowledge gap that must be addressed to support the effective development and application of EK-based soil and groundwater remediation technologies at the field-scale.

Electrokinetic Theory

Electromigration is the most effective transport mechanism to deliver a charged amendment through an electrolyte in an EK-dominated system. Theoretically electromigration can be influenced by the type of host material, insofar as this affects the spatial variation in properties of the porous media which control the applied EK phenomena. For homogeneous conditions the 1-D electromigration solute mass flux is given by Equation 1 (Acar and Alshawabkeh 1993):

$$J_i = C_i \, (u_i^* - k_e) \frac{\partial E}{\partial x} \tag{1}$$

where J_i is the electromigration mass flux of chemical species i (kg/m²/s); C_i, is the solute concentration (kg/m³); u_j^* is the effective ionic mobility (m²/V/s); k_e is the electroosmotic permeability (m²/V/s); E is the electrical potential (V); and x is distance (m). The effective ionic mobility is analogous to the effective diffusion coefficient (Equation 2):

$$u_i^* = u_i \, n \, \tau = \frac{D_i^* z_i F}{RT} \tag{2}$$

where n is porosity (—); τ is tortuosity (—); F is the Faraday's constant (C/mol); z is ion valence; D_i^* is the effective diffusion coefficient (m²/s); R is the universal gas constant

(J/K/mol); and T is absolute temperature (K). The effective solute diffusion coefficient has been shown to decrease with decreasing K due to a decrease in the tortuosity factor associated with the migration path length (Rowe and Badv 1996). From this relationship effective ionic mobility should also vary between sand, silts and clays, that is, decreasing with decreasing K. It is also likely that the counter pore fluid flux created by electroosmosis will increase with decreasing K, due to the presence of more fine grained particles with an associated larger surface charge, represented by the zeta potential (ζ) (Acar and Alshawabkeh 1993):

$$q_w = k_e \frac{\partial E}{\partial x} \tag{3}$$

$$k_e = \frac{\epsilon \zeta}{\eta} n \tag{4}$$

where q_w is the pore fluid flux (m/s); ϵ is the permittivity of the porous medium (C²/J/m); ζ is the zeta potential (V); and η is the fluid viscosity (Pa/s). For example, electroosmosis is about five times higher in clays than fine-grained sands with hydraulic conductivities of 1 to 2×10^{-8} m/s and 3.5×10^{-5} m/s, respectively (Wu et al. 2007). The electroosmotic flux is generally an order of magnitude lower than electromigration, and therefore electromigration is typically the dominant transport mechanism (Acar and Alshawabkeh 1993).

Under 1-D physically heterogeneous conditions where the porosity and tortuosity of the material vary and therefore the effective ionic mobility varies, there will be step changes in the electromigration velocity. Moreover, there should also be an associated variation in the voltage gradient due to the relationship between effective ionic mobility and effective electrical conductivity (Alshawabkeh and Acar 1996):

$$\frac{\partial E}{\partial x} = -\frac{I + F \sum_{i=1}^{N} z_i \, D_i^* \frac{\partial C_i}{\partial x}}{\sigma^*} \tag{5}$$

$$\sigma^* = \sum_{i=1}^{N} F \, z_i \, u_i^* \, C_i \tag{6}$$

where I is current density (C/s/m²); and σ^* is the effective fluid electrical conductivity (S/m).

Thus, in a physically heterogeneous setting where the concentration of chemical species is uniform, the voltage gradient should increase in material with a low effective ionic mobility relative to material with a high effective ionic mobility. This is in contrast to homogeneous systems where, if the effective ionic mobility and chemical species concentration are uniform, the voltage gradient is also uniform.

Materials and Methods

Material Properties

The porous medium was created using soda-lime-silica glass beads (Potters Ballotini Ltd, Barnsley, South Yorkshire, UK) and Speswhite kaolin (Imerys Performance Materials Ltd, Par, Cornwall, UK) to represent a model system composed of two materials with consistent properties.

The physical heterogeneity in these experiments is a contrast between high and low K, created by positioning layers of appropriate material in the test cell as shown in Figure 1. High hydraulic conductivity (HK) sections were consistently produced using 1.4 mm diameter glass beads, whereas low hydraulic conductivity (LK) sections were produced using a 90/10 mix of 0.25 and 0.5 mm glass beads. Between experiments the glass beads were cleaned with deionised water and autoclaved to minimise biological activity in the tests. Additional K contrasts were achieved by blending the small glass bead mix with different proportions by weight of kaolinite. The clay grain size distribution is 76% to 83% ≤ 2 μm and introduced a small amount of surface-adherent dissolvable salts (approximately 0.2% by mass of sodium and sulphate ions based on dissolution tests) into the test fluids.

Consolidation of glass beads in preparation for tests was achieved using a small shaker table at a frequency of 31 Hz and calibrated using a hand-held accelerometer. The test cells were filled with material in layers up to 3 cm and placed on the shaker table for intervals of 20 s. This was repeated until the test cell was full, excess material removed and the lid secured. The glass bead mix and clay was added together and combined with sterilised synthetic groundwater to give a mass equivalent to the clay's plastic limit (approximately 30% by weight of the clay). This was to facilitate mixing and aid compaction. The mixture was then wet packed into the sediment chamber in the test cell (Figure 1) and tamped down using a ceramic pestle, similar to the method used in Saichek and Reddy (2005b).

The K contrast was achieved by inserting a 0.5 mm thick stainless steel plate into vertical slots on the inside of the sediment chamber to separate the HK and LK sections. The material was then packed in the respective compartment either side of the plate, and the plate removed. This left a small space (approximately 0.5 mm wide) that was then back-filled by further consolidation. The lid was secured before the material was saturated with synthetic groundwater. The sediment chamber was separated from the electrode chambers by a perforated acrylic plate covered with filter paper (Whatman Grade No. 5), the aperture of which was less than the grain size of sediment used in the experiment.

A synthetic groundwater was used to simulate an electrical conductivity of 700 μS/cm, similar to natural groundwater sampled in a UK Aquifer (Thornton et al. 1995). This was achieved using a NaCl-deionised water solution to give 0.3 g-NaCl/L. Prior to adding NaCl deionised water was run through a tangential flow filtration unit (aperture 1 μm) to remove bacterial cells and minimise biological activity during tests. The test cells containing the consolidated material were saturated with synthetic groundwater from the base up to remove any trapped air. Saturation was considered complete when water was observed to emerge from 12 evenly spaced ports in the lid; these were then sealed.

Bench-Scale Setup

A 1-D experimental test cell was developed for the preparation of reproducible sections of packed materials with high and low K (Figure 1). The test cell was constructed from Perspex panels which were fixed together and sealed with silicone sealant. It comprised three main components: (1) a partitioned rectangular cell with compartments for the sediment and electrode chambers (H: 125 x W: 125 x L: 720 mm); (2) a lid that secured onto the rectangular cell with holes over the electrode chambers (H: 10 x W: 125 x L: 720 mm); and (3) a pair of electrode chamber header tanks that secured onto the lid to expand the volume of the electrode chambers and raise the water level above the sediment section (H: 160 x W: 125 x L: 95 mm). Leaks were prevented using rubber gaskets and silicone grease for the lid and header tanks. Once material was consolidated within the test cell and the lid and header tanks secured synthetic groundwater and the amendment solution was circulated using a peristaltic pump (Ismatec, REGLO MS-4/8) from the reservoir tank into the cathode chamber at 10 mL/min. This was done until the fluid in the cathode chamber had been displaced (approximately 3.5 h); at this point a Mariotte bottle was added to the anode chamber to minimise any hydraulic head difference between electrodes caused by electroosmotic flow and a baseline sample was taken. After this a direct current was applied to the system from a power pack (Digimess, Stenton, Derby, UK, PM6003-3). Constant current was established and checked with a multimeter (Digitek, Tsuen Wan, Hong Kong, China, DT-4000ZC).

Samples of the pore fluid for chemical analysis were taken every 2 to 4 days during the experiment via nine narrow bore (ID = 0.5 mm) PEEK tubes located along the length of the test chamber. The sampling tubes extended normal from the edge into the centre of the sediment mass within the test chamber and were offset to each other on either side of chamber. This ensured that any edge effects from the chamber panels on fluid sampling were avoided and that the centreline of the fluid flow path could be sampled in detail. Sample tube blockages were prevented by fitting a small cube of porous sintered glass to the end of each tube. At each time point seven samples of the pore fluid in the sediment chamber and one sample from each electrode chamber were taken. Each pore fluid sample was 1 mL to ensure that at each time point the total fluid extracted was <1% of the total pore fluid volume, with minimal disturbance.
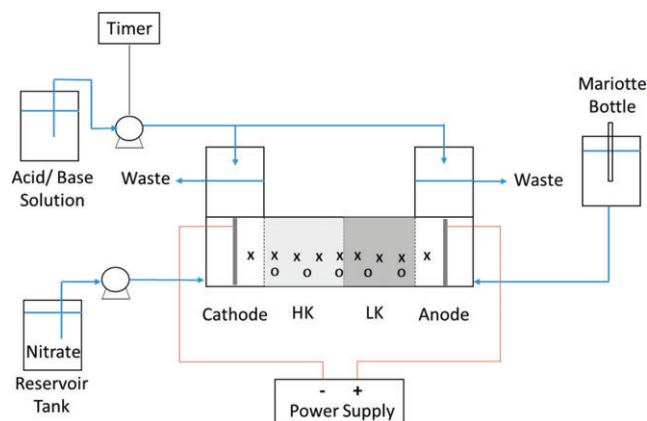

Figure 1. Schematic of experimental set-up used in tests. Sediment chamber volume: 7.5 L; and electrode chamber 2 L. HK and LK represent the high and low K contrasts in the sediment, X and O represent sampling and voltage probe ports.

Five voltage probes consisting of 4 mm diameter grade 316 stainless steel rods housed in HDPE piping were fitted within the chamber. Voltages and current were logged every 24 h or after sampling during the tests. The dimensions of the HK and LK sections were H:125 × W:125 × L:280 mm and H:125 × W:125 × L:210 mm, respectively; the difference accommodates the distribution of sample and voltage probe ports (Figure 1).

Nitrate was selected as it is a representative amendment used extensively in electrokinetic-bioremediation studies (Gill et al. 2014). Bromide was used as a tracer under an electric field because it is chemically conservative and has similar electromigration transport properties to nitrate. Amendments were added to the cathode at a rate 1.5 mL/min from a 10-L reservoir tank maintained at a constant concentration of either nitrate or bromide solutions. The reservoir tank was topped up at regular intervals.

Electrokinetic Apparatus and Test Conditions

A direct current was applied at a constant current strength of 25 mA (1.6 A/m^2) to allow more effective control of pH changes at the electrodes. Electrodes were made from a 125 × 125 × 10 mm graphite block perforated with 8 mm diameter holes to allow passage of water, using the method described by Harbottle et al. (2009). The connection between the graphite electrodes and copper wires to the DC power source was housed inside the electrodes and secured in place with a threaded seal and silicone sealant to give a water-tight seal. This also reduced the risk of contaminating the electrode chambers by metal corrosion.

A peristaltic pump (Ismatec, Mondfeld, Wertheim, Germany, Ecoline VC-MS/CA 8-6) was used to circulate acid and base solutions (1 M HCl and NaOH) to the cathode and anode, respectively, to neutralise electrolysis reactions as follows:

$$2H_2O - 4e^- \rightarrow 4H^+ + O_2 \qquad (7)$$

$$4H_2O + 4e^- \rightarrow 4OH^- + 2H_2 \qquad (8)$$
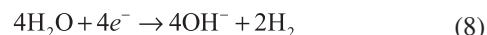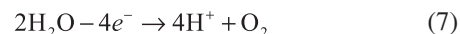
The rate of acid (H$^+$) and base (OH$^-$) generation can be estimated assuming steady-state electrolysis and 100% Faradaic efficiency at the electrode (Kim and Han 2003):

$$J_{HK} = C_{CATHODE} u^*_{HK} \frac{\partial E_{HK}}{\partial x_{HK}} \qquad (9)$$

where R_{H^+} is the rate of H$^+$ (or OH$^-$) generated (mol/s). These values were used to determine the volume of acid or base that would be required over a certain time period to neutralise electrolysis reactions, dosing being controlled by a timer and applied every 3 h. In experiments where electroosmotic flow was evident a Mariotte bottle was used to ensure that the anode compartment was not depleted of water and no hydraulic gradient developed.

Experimental Design

Two types of experiments were undertaken: (1) bromide tracer tests to determine the effective ionic mobility of the materials used in the HK and LK sections; and (2) nitrate migration experiments under homogeneous and heterogeneous conditions, based on the arrangement of materials used in the respective tests. Bromide tracer experiments were run under homogeneous conditions using the same material specifications used in the nitrate migration experiments (Table 1). Bromide was added at 1 g-Br/L concentration in the reservoir tanks, with fluid samples and voltage readings taken every 24 h. Nitrate migration experiments

Table 1

Design of Bromide Tracer and Nitrate Migration Experiments in Homogeneous (HOM) and Heterogeneous (HET) Conditions

| Name | EK Properties | | Reservoir Tank Properties | | HK Properties | | LK Properties/HOM Properties | | | | Duration (h) |
	Current Applied	Current (mA)	Ion	Conc (g/L)	n^*	K^2 (m/s)	n^1	Clay (%)	K^2 (m/s)	Reps	
Tracer_1	Yes	25	Br$^-$	1	—	—	0.29	—	2.2×10^{-4} ($\pm 2.1 \times 10^{-5}$)	1	192
Tracer_2	Yes	25	Br$^-$	1	—	—	0.37	—	1.5×10^{-5} ($\pm 1.6 \times 10^{-6}$)	1	192
Tracer_3	Yes	25	Br$^-$	1	—	—	0.29	5	1.6×10^{-6} ($\pm 2.7 \times 10^{-7}$)	1	240
Tracer_4	Yes	25	Br$^-$	1	—	—	0.34	10	1.2×10^{-7} (2.4×10^{-7})	1	240
Tracer_5	Yes	25	Br$^-$	1	—	—	0.41	20	4.5×10^{-9} (1.1×10^{-9})	1	263
Control_1	Yes	25	—	—	0.29	2.2×10^{-4} ($\pm 2.1 \times 10^{-5}$)	0.37	—	1.5×10^{-5} ($\pm 1.6 \times 10^{-6}$)	1	192
Control_2	No	—	NO$_3^-$	0.1	0.29	2.2×10^{-4} ($\pm 2.1 \times 10^{-5}$)	0.37	—	1.5×10^{-5} ($\pm 1.6 \times 10^{-6}$)	1	192
HOM	Yes	25	NO$_3^-$	0.1	0.29	—	0.37	—	1.5×10^{-5} ($\pm 1.6 \times 10^{-6}$)	2	192
HET_1	Yes	25	NO$_3^-$	0.1	0.29	2.2×10^{-4} ($\pm 2.1 \times 10^{-5}$)	0.37	—	1.5×10^{-5} ($\pm 1.6 \times 10^{-6}$)	3	192
HET_2	Yes	25	NO$_3^-$	1	0.29	2.2×10^{-4} ($\pm 2.1 \times 10^{-5}$)	0.37	—	1.5×10^{-5} ($\pm 1.6 \times 10^{-6}$)	2	192
HET_3	Yes	25	NO$_3^-$	1	0.29	2.2×10^{-4} ($\pm 2.1 \times 10^{-5}$)	0.29	5	1.6×10^{-6} ($\pm 2.7 \times 10^{-7}$)	1	288
HET_4	Yes	25	NO$_3^-$	1	0.29	2.2×10^{-4} ($\pm 2.1 \times 10^{-5}$)	0.34	10	1.2×10^{-7} (2.4×10^{-7})	1	288
HET_5	Yes	25	NO$_3^-$	1	0.29	2.2×10^{-4} ($\pm 2.1 \times 10^{-5}$)	0.41	20	4.5×10^{-9} (1.1×10^{-9})	1	288

[1]Averaged value.
[2]Falling head permeameter tests.

were run at low- and high-nitrate inlet concentrations of 0.1 and 1 g-NO$_3$/L, respectively. At low concentration nitrate migration was compared under heterogeneous and homogeneous conditions, whereas at high concentration nitrate migration was evaluated for increasing K contrasts (Table 1). Two control experiments with no nitrate and no direct current (Control_1 and Control_2, respectively) were also performed. The experimental results were interpreted according to theoretical predictions using numerical analysis of nitrate breakthrough at the anode (Equation 1) and proportion of the voltage gradient distributed across HK and LK sections based on major ion analysis (Equations 5 and 6). Replicates were run for experiments with low nitrate inlet concentration, HET_1, HOM, and high inlet concentration, HET_2. Experimental reproducibility is inferred from tests with one or more replicates. All experiments were run with pH control to eliminate the influence of acid and base fronts on the voltage gradient (Lohner et al. 2008).

Analytical Methods

Water samples taken from migration experiments were analysed for major ions (nitrate, bromide, chloride, sulphate, sodium, and potassium) using a Dionex (Hemel Hempstead, Hertfordshire, UK) DX-120 ion chromatograph. This allowed the quantification of the main components in the electrolyte. The anion column was an AS14A with a mobile eluent consisting of 8 mM sodium carbonate and 1 mM sodium bicarbonate at a flow rate of 1.34 mL/min. The cation column was an CS12A with a mobile eluent of 20 mM methane sulphonic acid at a flow rate of 1.05 mL/min. Calibration standards were run at the beginning of each batch and quality control standards were included every 15 samples. The maximum and minimum detection limits for the ions analysed were: 0.8 mg/L (sulphate) and 0.1 mg/L (sodium); and analytical precision: ±5.9% (potassium) and ±2.0% (bromide). Samples were also analysed for pH and electrical conductivity using ion selective electrodes and standard methods.

Results and Discussion

Bromide Electromigration under Homogeneous Conditions

Tracer experiments were conducted using bromide to determine the effective ionic mobility of nitrate for the different materials evaluated in the nitrate migration experiments This is justified as bromide has similar transport properties to nitrate under an electric field, for example both have similar ionic mobility at infinite dilution (bromide: 8.1×10^{-8} m^2/s/V; nitrate: 7.4×10^{-8} m^2/s/V; CRC 2002). A tortuosity factor for the host material was estimated from the effective ionic mobility of bromide to deduce the effective ionic mobility of nitrate (Equation 2).

Results from the bromide tracer experiments at steady-state are shown in Table 2. Steady-state in these experiments is the point at which nitrate breaks through to the anode and the mass transport normalised to the voltage gradient stops increasing. Mass transport is defined as the mass of bromide that passed through the sediment over time, normalised to the voltage gradient. The mass flux and effective ionic mobility can be determined from this value by re-arranging Equation 1. The tortuosity factor reflects the path length that ions must take through the sediment, in porous media it is always less than one and decreases as the tortuosity of the flow path increases (Fetter 1993); it is calculated by re-arranging Equation 2. The migration velocity is the distance across the sediment chamber divided by the time bromide is first observed in the anode chamber and is normalised to the voltage gradient.

Values for mass transport, effective ionic mobility and migration velocity all decrease with decreasing K (Table 2), with the exception of values for Tracer_1 which are slightly lower than Tracer_2. K and the effective ionic mobility have no direct relationship, as both reflect the porous material used. Results from these experiments demonstrate that these two parameters can be indirectly related by the tortuosity factor, which decreases in fine grained sediments (Rowe and Badv 1996). Thus, as K decreases the effective ionic mobility also decreases. For example, as clay content increases between Tracer_2 and Tracer_5 there is greater occlusion of the pore spaces between the larger glass beads, which impedes solute migration. The effective ionic mobility estimated for nitrate in the different materials is similar in trend to, but slightly lower than, the bromide results due to the differences in ionic mobility value at infinite dilution (Table 2). This range of values is lower than those reported for pure kaolin (1.55 to 1.65×10^{-8} m^2/V/s), which has high porosity and tortuosity values (0.6 and 0.35, respectively) (Acar and Alshawabkeh 1993; Thevanayagam & Rishindran 1998).

Electromigration of negative species such as bromide and nitrate towards the anode can be hindered by a counter electroosmotic flow in fine-grained material with a high

Table 2
Bromide Transport Properties at Steady-State Estimated from Tracer Tests

Experiment	Bromide Mass Transport [(m/s)/(V/m)]	Bromide Effective Ionic Mobility (m²/V/s)	Tortuosity Factor (—)	Migration Velocity [(m/s)/(V/m)]	Nitrate Effective Ionic Mobility (m²/V/s)
Tracer_1	7.0×10^{-5} ($\pm 3.5 \times 10^{-6}$)	1.4×10^{-8} ($\pm 1.1 \times 10^{-9}$)	0.56 (± 0.04)	6.3×10^{-8}	1.3×10^{-8} ($\pm 1.0 \times 10^{-9}$)
Tracer_2	7.9×10^{-5} ($\pm 7.5 \times 10^{-6}$)	1.5×10^{-8} ($\pm 1.6 \times 10^{-9}$)	0.55 (± 0.06)	5.0×10^{-8}	1.4×10^{-8} ($\pm 1.5 \times 10^{-9}$)
Tracer_3	5.8×10^{-5} ($\pm 6.8 \times 10^{-6}$)	1.1×10^{-8} ($\pm 1.5 \times 10^{-9}$)	0.47 (± 0.06)	4.1×10^{-8}	1.0×10^{-8} ($\pm 1.3 \times 10^{-9}$)
Tracer_4	4.5×10^{-5} ($\pm 4.4 \times 10^{-6}$)	8.2×10^{-9} ($\pm 7.5 \times 10^{-10}$)	0.30 (± 0.03)	4.4×10^{-8}	7.5×10^{-8} ($\pm 6.9 \times 10^{-10}$)
Tracer_5	2.5×10^{-5} ($\pm 1.2 \times 10^{-7}$)	7.2×10^{-9} ($\pm 5.4 \times 10^{-11}$)	0.22 (± 0.002)	1.5×10^{-8}	6.5×10^{-8} ($\pm 4.9 \times 10^{-11}$)

Mass transport and migration velocity are normalised against the voltage gradient. The error represents one standard deviation from the mean of values obtained once the experiment has reached steady-state.

surface charge (Acar and Alshawabkeh 1993). Other authors have noted this phenomena, whereby a negatively charged ion migrates faster through sands than clays due to the presence of counter electroosmotic flow (Acar et al. 1997; Wu et al. 2007). In these experiments electroosmotic flow was only observed in Tracer_5, with a 20% clay content (electroosmotic permeability: 2.7×10^{-9} ($\pm 3.6 \times 10^{-10}$) $m^2/V/s$) because all systems are run at constant current where the voltage gradient decreases over time. Under these conditions the ratio between electromigration and electroosmosis increases over time and the influence of electroosmotic flow decreases (Acar and Alshawabkeh 1993).

Nitrate Electromigration under Heterogeneous Conditions

Observed and calculated values for nitrate breakthrough at the anode in experiments HET_1, HOM and HET_2 are shown in Figure 2. HET_1 and HOM experiments were run at an inlet concentration of 0.1 g/L under heterogeneous and homogeneous configurations, whereas HET_2 is the same heterogeneous configuration to HET_1 but with an inlet concentration of 1 g/L. Results in Figure 2 are normalised to the starting inlet concentration and the voltage gradient across the length of the sediment section. Calculated values for the HOM experiment were obtained using Equation 1 for 1-D electromigration, whereas values for heterogeneous experiments can be calculated by modifying this equation to account for migration through the HK and LK sections:

$$J_{HK} = C_{CATHODE}\, u^*_{jHK}\, \frac{\partial E_{HK}}{\partial x_{HK}} \qquad (10)$$

$$J_{LK} = C_{HK}\, u^*_{jLK}\, \frac{\partial E_{LK}}{\partial x_{LK}} \qquad (11)$$

where J_{HK} and J_{LK} are the mass flux across the HK and LK sections, $C_{Cathode}$ and C_{HK} are the concentrations in the cathode compartment and HK section; x_{HK} and x_{LK} are the distances across the sections; and E_{HK} and E_{LK} are the electrical

potentials across the different sections. Equation 10 represents the mass flux of nitrate from the cathode into the HK section accounting for the effective ionic mobility of the material and voltage gradient across that section. Equation 11 incorporates the same variables for the LK section but uses the nitrate concentration within the HK section calculated from the mass flux in Equation 10. Calculated values are derived from the effective ionic mobility determined in the bromide tracer experiments, observed voltage gradient and inlet nitrate concentration values (either 0.1 or 1 g/L). This method was used to calculate the nitrate concentration at the anode over time. Good agreement between the observed and calculated values shows that the observed experimental values conform to applicable EK theory (Figure 2).

The observed nitrate breakthrough for HET_1 is higher than HOM and HET_2 after 100 h, relative to the inlet concentration and voltage gradient (Figure 2). A good match between observed and calculated datasets shows that this is due to a higher voltage gradient across the HK section in HET_1 (Figure 3A). This allows more nitrate to enter the sediment section from the cathode and increase the proportion passed through the LK section, relative to HOM and HET_2.
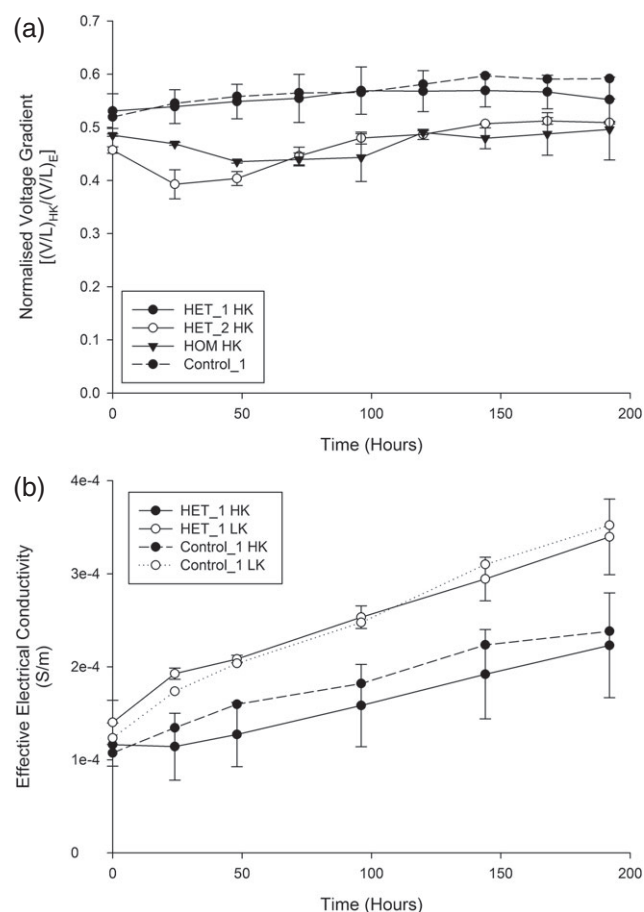
Figure 3. (A) Proportion of voltage gradient across the HK section for HET_1, Control_1 and HET_2 and the equivalent section in the HOM experiment. (B) Effective electrical conductivity for the HK and LK sections in HET_1 and Control_1 calculated using Equation 6 and the ionic composition of the pore fluid from sample ports in the respective sections. Error bars for values from experiments HET_1 and HET_2 represent one standard deviation from the mean between replicates.
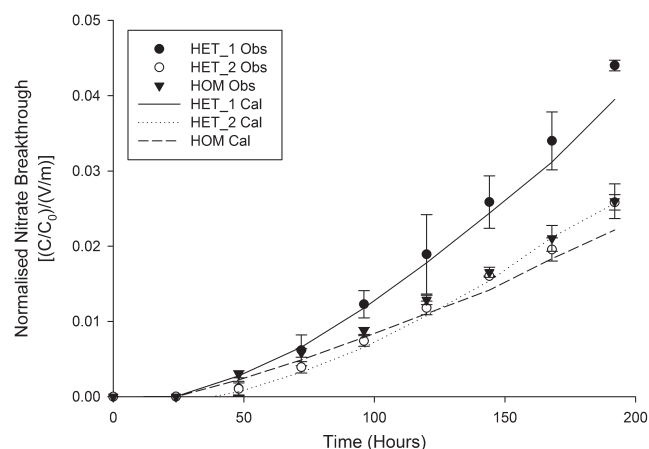
Figure 2. Nitrate breakthrough at the anode normalised to inlet concentration and voltage gradient across the sediment section for experiments HET_1, HOM and HET_2. Dots and dashed lines represent the observed and calculated values, respectively. Error bars represent one standard deviation from the mean; error associated with the calculated values is within the same range for observed values.

The increased voltage gradient across the HK section in HET_1 can be attributed to several factors. Firstly, the effective ionic mobility has an inverse relationship with the voltage gradient (Equations 5 and 6). In these experiments the effective ionic mobility is slightly lower in the HK section compared with the LK section (Table 2). Therefore, there should be an elevated voltage gradient across the HK section, which is evident for both HET_1 and Control_1 in Figure 3A. This phenomena is the likely cause for the divergence in effective electrical conductivity between the HK and LK sections of HET_1 and Control_1 in Figure 3B. Ions will move faster through the HK section where the voltage gradient is highest but accumulate in the LK section where it decreases and electromigration rate subsequently falls. Li et al. (2013) noted similar phenomena when investigating the influence of bands with a high associated electrical conductivity within a homogeneous soil. They found that the associated decrease in the voltage gradient caused the electromigration rate to fall. Over time these bands dissipated due to chemical diffusion, but in physically heterogeneous settings the contrast in migration rates could establish a permanent change in the voltage gradient.

Secondly, between HET_1 and HET_2 nitrate accounts for different proportions of the total electrolyte. Based on Equation 6 and accounting for the major ions in the electrolyte, nitrate in HET_1 is 3.4% (± 0.4%) when added at 0.1 g/L compared with HET_2, where it accounts for 22.8% (± 2.3%) when added at 1 g/L. Therefore nitrate should have a greater effect on the voltage gradient in HET_2 compared with HET_1. This is observed in Figure 3A, where the voltage gradient across the HK system dips for HET_2 over the first 100 h due to nitrate entering the system and increasing the electrical conductivity of the electrolyte in that zone. This phenomena is noted by Wu et al. (2012a), who found that increasing the concentration of the amendment in homogeneous settings increased the depression in the voltage gradient adjacent to the cathode and thus reduced the relative amount of amendment that migrated into the material.

Nitrate Electromigration under an Increasing Hydraulic Conductivity Contrast

Experiments HET_2 to HET_5 quantify the effect of an increasing contrast in the *K* between two host materials on the electromigration of nitrate through them. The transport properties of nitrate through HK and LK sections of the sediment are in broad agreement with the bromide tracer results from homogeneous settings (Table 3). For example, the range in HK mass transport and migration velocity values (except HET_5) are equivalent to Tracer_1 and the trend in decreasing mass transport and migration velocity between Tracer_2 to Tracer_5 is repeated in the LK results. In addition, electroosmotic flow is observed in HET_5 that originates in the LK section and transfers through the HK section, contributing to the relatively low mass transport value; migration velocity is not restricted because nitrate was detected in the LK section after 24 h. However mass transport estimates are either equivalent to, or higher in, the LK section compared with the relevant bromide tracer experiment. This results from the influence of the voltage gradient on the heterogeneous setting.

Furthermore, nitrate concentration in the HK section increases as the ratio between HK/LK sections increases (Figure 4). This is due to a reduction in electromigration rates from the HK to LK sections. The range of values for steady-state concentrations under homogenous conditions are shown as dotted lines and show the expected conditions without the associated influences of a heterogeneous system. These are calculated using the method in Wu et al. (2012a), applying the bromide mass transport values from experiment Tracer_1 (Table 2). Results for HET_2 are closest to the steady-state nitrate concentration because the HK and LK effective ionic mobility values are closest. Conversely, HET_5 values are furthest from steady-state due to the combined effect of a low associated effective ionic mobility in the LK section and counter electroosmotic flow, which hinders nitrate migration.

Influence of Increasing Hydraulic Conductivity Contrasts on the Voltage Gradient

EK-driven mass transport increases in heterogeneous relative to homogeneous systems (Tables 2 and 3), for example the mass transport for HET_4 is 7.4×10^{-5} ($\pm 1.1 \times 10^{-5}$) compared with 4.5×10^{-5} ($\pm 4.4 \times 10^{-6}$) (mg/s)/(V/m) in equivalent material for Tracer_4. This is because in heterogeneous settings the voltage gradient is higher across the zone with a low effective ionic mobility compared with a homogeneous setting where the voltage gradient is more

Table 3

Nitrate Transport Properties at Steady-State for Experiments HET_2 to HET_5 Quantifying the Effect of Increasing K Contrasts on Nitrate Migration

| Experiment | HK Transport Properties | | LK Transport Properties | | |
	Mass Transport [(m/s)/(V/m)]	Migration Velocity [(m/s)/(V/m)]	Mass Transport [(m/s)/(V/m)]	Migration Velocity [(m/s)/(V/m)]	Electroosmotic Permeability (m²/V/s)
HET_2A	8.4×10^{-5} ($\pm 1.4 \times 10^{-5}$)	4.6×10^{-8}	8.2×10^{-5} ($\pm 8.6 \times 10^{-6}$)	3.4×10^{-8}	—
HET_2B	8.6×10^{-5} ($\pm 1.9 \times 10^{-5}$)	6.4×10^{-8}	8.8×10^{-5} ($\pm 1.3 \times 10^{-5}$)	3.9×10^{-8}	—
HET_3	9.3×10^{-5} ($\pm 2.0 \times 10^{-5}$)	4.6×10^{-8}	8.6×10^{-5} ($\pm 1.3 \times 10^{-5}$)	3.0×10^{-8}	—
HET_4	1.0×10^{-4} ($\pm 1.4 \times 10^{-5}$)	4.7×10^{-8}	7.4×10^{-5} ($\pm 1.1 \times 10^{-5}$)	3.8×10^{-8}	—
HET_5	5.8×10^{-5} ($\pm 2.5 \times 10^{-6}$)	5.3×10^{-8}	3.8×10^{-5} ($\pm 7.3 \times 10^{-6}$)	1.3×10^{-8}	3.8×10^{-9} ($\pm 6.4 \times 10^{-10}$)

The error represents one standard deviation from the mean of values obtained once the experiment has reached steady-state. Both replicates for HET_2 are shown.
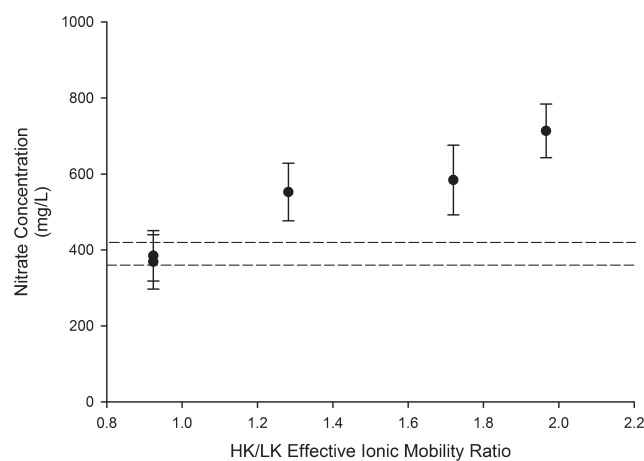
Figure 4. Nitrate concentration in the HK material at steady-state, calculated from the total mass of nitrate detected in the sample ports along the HK section and divided by the domain volume. Lines plotted at nitrate concentrations of 412 and 373 mg/L represent the maximum and minimum steady-state concentration calculated using values for equivalent material from the bromide tracer experiment. The error bars represent one standard deviation from the mean of values at steady-state.

Table 4

Percentage Change in the Voltage Gradient Across the HK and LK Sections at Steady-State Relative to a Fixed Voltage Gradient

Experiment	HK/LK Effective Ionic Mobility Ratio	HK Section	LK Section
HET_2A	0.92	−0.7% (± 3.9%)	0.7% (± 3.9%)
HET_2B	0.92	0.3% (± 2.0%)	−0.3% (± 2.0%)
HET_3	1.28	−19.6% (± 3.0%)	19.6% (± 3.0%)
HET_4	1.72	−18.5% (± 2.0%)	18.5% (± 2.0%)
HET_5	1.97	−30.1% (±1.6%)	30.1% (±1.6%)

The error represents one standard deviation from the mean of values obtained once the experiment has reached steady-state. Both replicates for HET_2 are shown.

uniform. These experiments show that increasing the K and associated effective ionic mobility contrast increases the difference in voltage gradient between the HK and LK sections (Table 4). In experiments with a low effective ionic mobility contrast (HET_2) the observed voltage gradient is distributed evenly, that is, there is little change in the voltage gradient across the HK and LK zones relative to a uniform voltage gradient. At higher K contrasts there is a difference of up to 30% relative to a fixed voltage gradient (HET_5). The factors controlling this difference can be identified from Equations 5 and 6 as the spatial change in effective ionic mobility and subsequent spatial change in the effective electrical conductivity. Additionally, the spatial change in migration rates resulting from changes in the effective ionic mobility will influence the distribution of ions within the system.

A comparison of the major ion concentrations in the electrolyte (nitrate, chloride, sulphate, sodium and potassium) across two different K contrasts highlights the complex
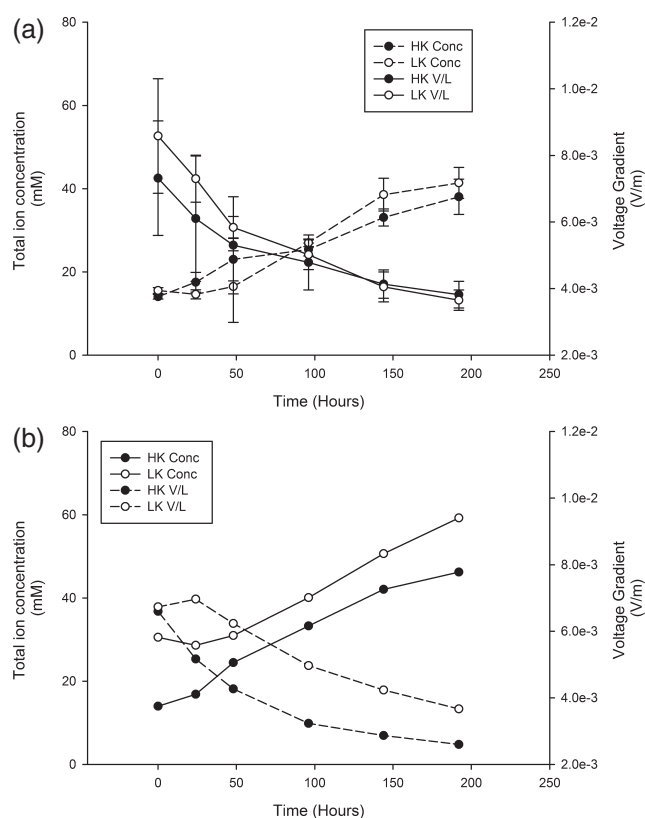

Figure 5. Total ion concentrations and voltage gradient (VG) for experiments (A) HET_2 and (B) HET_4. Values for the total ion concentration are calculated from the cumulative mass of each ion identified at sample ports along the HK and LK sections divided by the volume of the domain. These values are in mM because five different ions are included in the analysis. Error bars on (A) represent one standard deviation from the mean between replicates.

interactions between the effective ionic mobility and the voltage gradient in heterogeneous settings (Figure 5). In experiment HET_2 there is minimal difference between the total ion concentration and voltage gradient (Figure 5A). However, in HET_4 there is a higher total ion concentration in the LK zone compared with the HK zone (Figure 5B). Assuming uniform effective ionic mobility (and according to Equation 5) this should be reflected by a higher voltage gradient across the HK section relative to the LK section because there is a lower concentration and therefore a lower electrical conductivity. However, the opposite is observed due to the difference in effective ionic mobility. This demonstrates that under heterogeneous conditions where ionic mobility varies spatially there will be associated changes in the voltage gradient.

Experiment Mass Balance

As a quality control check on the operation of the experiments a mass balance for nitrate was undertaken, by comparing the mass of nitrate recovered at the end of the experiment with the known input (Table 5). The amount of amendment recovered (80% to 90%) is similar to that found in other electrokinetic transport experiments (73% to 106%) (Wu et al. 2007; Lohner et al. 2008). Every effort was made to minimise the loss of nitrate via biological processes

Table 5

Nitrate Mass Balance at the End of the Experiment Run for HET_2 to HET_5

| Experiment | Mass Balance | | |
	Mass In (mg)	Mass Recovered (mg)	Recovery (%)
HET_2A	4984	4422	89
HET_2B	4582	4119	90
HET_3	5907	5271	89
HET_4	6536	5215	80
HET_5	4644	4067	88

(e.g., denitrification), by sterilising glass beads, synthetic groundwater and test cell components to kill any microorganisms present. The mass balance suggests this loss was limited to 10% to 20% in these experiments.

Implications for Field–Scale Application

This study demonstrates that electrokinetic phenomena can enhance the transfer of amendments across a permeability boundary. The important implication for field applications is the observation that LK zones cause an increase in the voltage gradient across that zone. Scaling up these findings requires consideration of several factors shown in Figure 6. This scenario assumes that the contamination is localised within the LK zone and an amendment is added at the cathode and migrated towards the anode. It is representative of scenarios where EK is applied to a heterogeneous subsurface.

Physical heterogeneity will directly affect the choice of electrode configuration, as this influences the electric field. There are numerous types of electrode configuration, the two considered here are unidirectional (shown in Figure 6) and radial arrangements. Under a unidirectional configuration with a simple K contrast at the field-scale, similar phenomena to those observed in these experiments will occur.
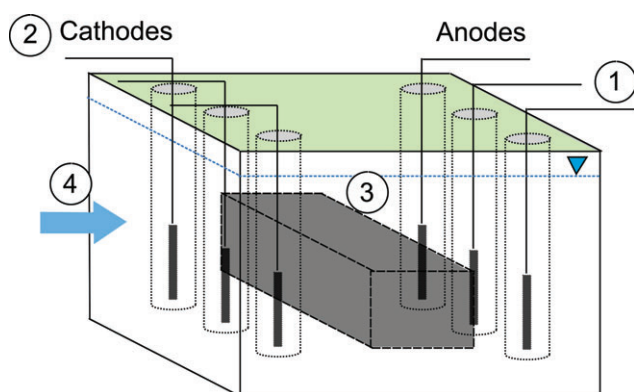

Figure 6. onceptual model of electrokinetic remediation applied to a contaminated LK zone (gray block) within a HK host porous media. Labels refer to the aspects of the treatment that are relevant to consider for upscaling to the field: 1, electrode configuration and spacing; 2, amendment properties; 3, properties of the LK zone; and 4, interactions with groundwater flow.

However, if the variety and orientation of LK zones varies there will be corresponding perturbations to the applied electric field. A nonlinear electric field results in nonlinear ion flow paths, decreasing migration rates between electrodes (Segall and Bruell 1992). A radial configuration consists of a central electrode surrounded by electrodes of the opposite polarity. In these settings the voltage gradient tends to be highest adjacent to the central electrode (Alshawabkeh et al. 1999). This could be enhanced in heterogeneous settings by placing this central electrode within a LK zone and the surrounding electrodes within the HK host material. An increase in the spacing between the anode and cathode results in higher predicted energy expenditure and remediation times (Alshawabkeh et al. 1999). In the experiments in this paper, heterogeneity affected the voltage gradient in a consistent manner, indicating that the influence of heterogeneity will be independent of the spacing between electrodes.

Selecting the right amendment concentration for a treatment requires consideration of several factors and the trade-offs between them. If amendment concentration is too high, migration will stall adjacent to the electrode (Wu et al. 2012a), however, if it is too low insufficient amendment mass will be delivered to the contaminated zone (Rabbi et al. 2000). Experiments in this paper demonstrate that, under heterogeneous conditions, the voltage gradient is highest across the LK zone in a system with a high K contrast. If amendments were added into these LK zones via electrode or amendment wells, the higher voltage gradient would counter the effect of the voltage gradient drop associated with adding high amendment concentrations. Thus, a higher amendment mass flux into the sediment could be maintained compared to a homogenous setting. For example, in clay an amendment concentration equivalent to 0.2 S/m at an electrode spacing of 1 m results in a 60% drop in the voltage gradient next to the cathode compared to a system where the voltage gradient is fixed (Wu et al. 2012a). Assuming a system where 100 V is applied between electrodes 1 m apart and homogeneous conditions where voltage is distributed uniformly the inlet voltage gradient decreases from 100 V/m to 40 V/m. In a heterogeneous setting where an increase of 30% relative to a fixed voltage gradient is observed across a LK zone equivalent to half the sediment section (Table 4), the voltage gradient would drop from 130 V/m to 52 V/m.

The type of K contrast will influence the effect on the voltage gradient. For example, a graduated contrast from LK to HK could cause a step-like increase in the voltage gradient. Alternatively a HK-LK-HK contrast as in Figure 6 would create an increase in the voltage gradient specifically over the LK zone. Furthermore, it is important to maximise current density against the surface area of the LK zone to enhance mass flux perpendicular to the electric field and increase treatment efficiency. For example, in Figure 6 the LK zone is normal to the direction of the electric field, exposing a large surface area to the amendment flux. However, in scenarios with multiple, narrow, LK (e.g., clay) lenses the treatment efficiency may drop because less amendment reaches the target location, with implications for treatment costs (Wu et al. 2012b).

An advective flow field will also have an important control on the configuration of an EK field setup. Advection will be more dominant in HK material, whereas EK will be more important in LK material. For example, calculated advective bromide mass flux (hydraulic gradient: 0.1; concentration: 1 g/L) in HK and LK materials is 2.2×10^{-2} and 4.5×10^{-7} g/m^2/s, respectively, compared with an observed bromide electromigration mass flux in HK and LK material of 1.2×10^{-4} and 7.4×10^{-5} g/m^2/s, respectively. In HK material solute transport by EK cannot easily override advection in the opposite direction (Eid et al. 1999). However, for treatments to be effective in scenarios such as Figure 6, an amendment must first migrate through the HK section to reach the target LK zone. The solution is to position the electric field so that it complements the existing advective flow field (as shown in Figure 6), or place the amendment injection well/ electrode within the LK zone, thus eliminating the influence of the advective flow field.

Conclusions

Physical heterogeneity in granular porous media, represented by a *K* contrast, exerts an important influence on the migration, under an electric field, of nitrate used as an amendment for bioremediation. In heterogeneous settings *K* contrasts reflect a spatial change in the effective ionic mobility, with subsequent control on the migration rate of an amendment and the distribution of the voltage gradient. The spatial change in migration rate leads to an accumulation of the amendment at the interface between high- and low-*K* zones, relative to the steady-state concentration. Moreover, in heterogeneous settings the voltage gradient is highest in zones where the effective ionic mobility is lowest. This leads to higher mass transport in LK zones within a heterogeneous setting relative to the same material in a homogeneous setting.

Overall these results show that EK application in heterogeneous settings is controlled by the same mechanisms in homogeneous settings, but that the distribution in amendment migration rates and voltage gradient vary relative to the change in the effective ionic mobility. These phenomena can be manipulated at the field-scale to either establish a high voltage gradient across the inlet zone, to increase the mass of amendment that enters the system, or ensure that a high voltage gradient is established across the zone targeted for bioremediation, to enhance biodegradation in situ. Thus, EK is not restricted in the heterogeneous configurations investigated in this study. Further work on the effectiveness of EK in heterogeneous systems should consider more complex heterogeneous configurations and attempt to quantify the effect of resulting non-uniform electric fields on amendment migration. In addition, EK experiments examining physical heterogeneity should be extended to include other variables, such as microorganisms for contaminant biodegradation, to determine their mobility under EK.

Acknowledgments

References

Acar, Y.B., M.F. Rabbi, and E.E. Ozsu. 1997. Electrokinetic injection of ammonium and sulfate ions into sand and kaolinite beds. *Journal of Geotechnical and Geoenvironmental Engineering* 123, no. 3: 239–249. doi:10.1061/(ASCE)1090-0241(1997)123:3(239).

Acar, Y.B., and A.N. Alshawabkeh. 1993. Principles of electrokinetic remediation. *Environmental Science & Technology* 27, no. 13: 2638–2647. doi:10.1021/es00049a002.

Alshawabkeh, A.N., and Y.B. Acar. 1996. Electrokinetic remediation. II: Theoretical model. *Journal of Geotechnical Engineering* 122, no. 3: 186–196. doi:10.1061/(ASCE)0733-9410(1996)122:3(186).

Alshawabkeh, A.N., A.T. Yeung, and M.R. Bricka. 1999. Practical aspects of in-situ electrokinetic extraction. *Journal of Environmental Engineering* 125, no. 1: 27–35. doi:10.1061/(ASCE)0733-9372(1999)125:1(27).

Bauer, R.D., P. Maloszewski, Y. Zhang, R.U. Meckenstock, and C. Griebler. 2008. Mixing-controlled biodegradation in a toluene plume – Results from two-dimensional laboratory experiments. *Journal of Contaminant Hydrology* 96, no. 1–4: 150–168. doi:10.1016/j.jconhyd.2007.10.008.

CRC. 2002. In *Handbook of Chemistry and Physics*, ed. D.R. Lide, 83rd ed. Boca Raton, Florida: CRC Press.

Eid, N., D. Larson, D. Slack, and P. Kiousis. 1999. Nitrate electromigration in sandy soil in the presence of hydraulic flow. *Journal of Irrigation and Drainage Engineering* 125, no. 1: 7–11. doi:10.1061/(ASCE)0733-9437(1999)125:1(7).

Fetter, C. 1993. Contaminant Hydrogeology. New York: Macmillan Publishing Company.

Gill, R.T., M.J. Harbottle, J.W.N. Smith, and S.F. Thornton. 2014. Electrokinetic-enhanced bioremediation of organic contaminants: A review of processes and environmental applications. *Chemosphere* 107: 31–42. doi:10.1016/j.chemosphere.2014.03.019.

Guo, S., R.F.T. Li, N. Hartog, F. Li, and X. Yang. 2014. Synergistic effects of bioremediation and electrokinetics in the remediation of petroleum-contaminated soil. *Chemosphere* 109. doi:10.1016/j.chemosphere.2014.02.007.

Harbottle, M.J., G. Lear, G.C. Sills, and I.P. Thompson. 2009. Enhanced biodegradation of pentachlorophenol in unsaturated soil using reversed field electrokinetics. *Journal of Environmental Management* 90, no. 5: 1893–1900. doi:10.1016/j.jenvman.2008.12.012.

Kim, S.S., and S.J. Han. 2003. Application of an enhanced electrokinetic ion injection system to bioremediation. *Water, Air, & Soil Pollution* 146: 365–377. doi:10.1023/A:1023934518049.

Lee, M.-K., J.A. Saunders, and L.W. Wolf. 2000. Effects of geologic heterogeneities on pump-and-treat and in situ bioremediation: A stochastic analysis. *Environmental Engineering Science* 17, no. 3: 183–189. doi:10.1089/ees.2000.17.183.

Li, D., Y.-Y. Niu, M. Fan, D.-L. Xu, and P. Xu. 2013. Focusing phenomenon caused by soil conductance heterogeneity in the electrokinetic remediation of chromium (VI)-contaminated soil. *Separation and Purification Technology* 120: 52–58. doi:10.1016/j.seppur.2013.09.018.

Li, L., C.I. Steefel, M.B. Kowalsky, A. Englert, and S.S. Hubbard. 2010. Effects of physical and geochemical heterogeneities on mineral transformation and biomass accumulation during biostimulation experiments at Rifle, Colorado. *Journal of Contaminant Hydrology* 112, no. 1–4: 45–63. doi:10.1016/j.jconhyd.2009.10.006.

Lohner, S.T., D. Katzoreck, and A. Tiehm. 2008. Electromigration of microbial electron acceptors and nutrients: (I) transport in synthetic media. *Journal of Environmental Science and Health. Part A, Toxic/hazardous Substances & Environmental Engineering* 43, no. 8: 913–921. doi:10.1080/10934520801974434.

Mao, X., J. Wang, A. Ciblak, E.E. Cox, C. Riis, M. Terkelsen, D.B. Gent, and A.N. Alshawabkeh. 2012. Electrokinetic-enhanced bioaugmentation for remediation of chlorinated solvents contaminated clay. *Journal of Hazardous Materials* 213–214: 311–317. doi:10.1016/j.jhazmat.2012.02.001.

McCray, J.E., G.R. Tick, J.W. Jawitz, J.S. Gierke, M.L. Brusseau, R.W. Falta, R.C. Knox, D.A. Sabatini, M.D. Annable, J.H. Harwell, and A.L. Wood. 2011. Remediation of NAPL source zones: Lessons learned from field studies at Hill and Dover AFB. *Ground Water* 49, no. 5: 727–744. doi:10.1111/j.1745-6584.2010.00783.x.

Niqui-Arroyo, J.-L., M. Bueno-Montes, R. Posada-Baquero, and J.-J. Ortega-Calvo. 2006. Electrokinetic enhancement of phenanthrene biodegradation in creosote-polluted clay soil. *Environmental Pollution* 142, no. 2: 326–332. doi:10.1016/j.envpol.2005.10.007.

Rabbi, M.F., B. Clark, R.J. Gale, E. Ozsu-Acar, J. Pardue, and A. Jackson. 2000. In situ TCE bioremediation study using electrokinetic cometabolite injection. *Waste Management* 20, no. 4: 279–286. doi:10.1016/S0956-053X(99)00329-3.

Rahman, M.A., S.C. Jose, W. Nowak, and O.A. Cirpka. 2005. Experiments on vertical transverse mixing in a large-scale heterogeneous model aquifer. *Journal of Contaminant Hydrology* 80, no. 3–4: 130–148. doi:10.1016/j.jconhyd.2005.06.010.

Reddy, K.R., and R.E. Saichek. 2003. Effect of soil type on electrokinetic removal of phenanthrene using surfactants and cosolvents. *Journal of Environmental Engineering* 129, no. 4: 336–346. doi:10.1061/(ASCE)0733-9372(2003)129:4(336).

Reynolds, D.A., and B.H. Kueper. 2002. Numerical examination of the factors controlling DNAPL migration through a single fracture. *Ground Water* 40, no. 4: 368–377. doi:10.1111/j.1745-6584.2002.tb02515.x.

Reynolds, D.A., E.H. Jones, M. Gillen, I. Yusoff, and D.G. Thomas. 2008. Electrokinetic migration of permanganate through low-permeability media. *Ground Water* 46, no. 4: 629–637. doi:10.1111/j.1745-6584.2008.00415.x.

Rowe, R.K., and K. Badv. 1996. Chloride migration through clayey silt underlain by fine sand or silt. *Journal of Geotechnical Engineering* 122, no. 1: 60–68. doi:10.1061/(ASCE)0733-9410(1996)122:1(60).

Saichek, R.E., and K.R. Reddy. 2005a. Electrokinetically enhanced remediation of hydrophobic organic compounds in soils: A review. *Critical Reviews in Environmental Science and Technology* 35, no. 2: 115–192. doi:10.1080/10643380590900237.

Saichek, R.E., and K.R. Reddy. 2005b. Surfactant-enhanced electrokinetic remediation of polycyclic aromatic hydrocarbons in heterogeneous subsurface environments. *Journal of Environmental Engineering and Science* 4, no. 5: 327–339. doi:10.1139/s04-064.

Segall, B.A., and C.J. Bruell. 1992. Electroosmotic contaminant-removal processes. *Journal of Environmental Engineering* 118, no. 1: 84–100. doi:10.1061/(ASCE)0733-9372(1992)118:1(84)

Song, X., E. Hong, and E.A. Seagren. 2014. Laboratory-scale in-situ bioremediation in heterogeneous porous media: Biokinetics-limited scenario. *Journal of Contaminant Hydrology* 158: 78–92. doi:10.1016/j.jconhyd.2014.01.001.

Song, X., and E.A. Seagren. 2008. In situ bioremediation in heterogeneous porous media: Dispersion-limited scenario. *Environmental Science & Technology* 42, no. 16: 6131–6140. doi:10.1021/es0713227.

Spence, M.J., S.H. Bottrell, J.J. Higgo, I. Harrison, and A.E. Fallick. 2001. Denitrification and phenol degradation in a contaminated aquifer. *Journal of Contaminant Hydrology* 53, no. 3–4: 305–318. http://www.ncbi.nlm.nih.gov/pubmed/11820475.

Thevanayagam, S., and T. Rishindran. 1998. Injection of nutrients and TEAs in clayey soils using electrokinetics. *Journal of Geotechnical and Geoenvironmental Engineering* 124, no. 4: 330–338. doi:10.1061/(ASCE)1090-0241(1998)124:4(330).

Thornton, S.F., D.N. Lerner, and J.H. Tellham. 1995. *The Technical Aspects of Controlled Waste Management: Laboratory Studies of Landfill Leachate-Triassic Sandstone Interactions*. London, UK: Department of the Environment.

Wu, M.Z., D.A. Reynolds, H. Prommer, A. Fourie, and D.G. Thomas. 2012a. Numerical evaluation of voltage gradient constraints on electrokinetic injection of amendments. *Advances in Water Resources* 38: 60–69. doi:10.1016/j.advwatres.2011.11.004.

Wu, M.Z., D.A. Reynolds, A. Fourie, H. Prommer, and D.G. Thomas. 2012b. Electrokinetic in situ oxidation remediation: Assessment of parameter sensitivities and the influence of aquifer heterogeneity on remediation efficiency. *Journal of Contaminant Hydrology* 136–137: 72–85. doi:10.1016/j.jconhyd.2012.04.005.

Wu, X., A.N. Alshawabkeh, D.B. Gent, S.L. Larson, and J.L. Davis. 2007. Lactate transport in soil by DC fields. *Journal of Geotechnical and Geoenvironmental Engineering* 133, no. 12: 1587–1596. doi:10.1061/(ASCE)1090-0241(2007)133:12(1587).

Xu, W., C. Wang, H. Liu, Z. Zhang, and H. Sun. 2010. A laboratory feasibility study on a new electrokinetic nutrient injection pattern and bioremediation of phenanthrene in a clayey soil. *Journal of Hazardous Materials* 184, no. 1–3: 798–804. doi:10.1016/j.jhazmat.2010.08.111.

Biographical Sketches

Richard T. Gill, BSc, corresponding author, is at Groundwater Protection & Restoration Group, University of Sheffield, Department of Civil & Structural Engineering, Kroto Research Institute, Broad Land, Sheffield S3 7HQ, UK; richard.gill@shef.ac.uk

Steven F. Thornton, BSc, PhD, is at Groundwater Protection & Restoration Group, University of Sheffield, Department of Civil & Structural Engineering, Kroto Research Institute, Broad Land, Sheffield, S3 7HQ, UK.

Michael J. Harbottle, MEng, PhD, is at Cardiff University, School of Engineering, Queen's Buildings, The Parade, Cardiff CF24 3AA, UK.

Jonathan W.N. Smith, BSc, MSc, PhD, is at Shell Global Solutions, Lange Kleiweg 40, 2288 GK Rijswijk, The Netherlands.